Vision Research 236 (2025) 108680

Contents lists available at ScienceDirect

Vision Research

journal homepage: www.elsevier.com/locate/visres

The contribution of magnocellular selective adaptation to spatial distance compression☆

Ljubica Jovanovic [a,b,*], Kristian Skoczek [a,c], Paul McGraw [a], Neil Roach [a], Alan Johnston [a]

[a] Visual Neuroscience Group, School of Psychology, University of Nottingham NG7 2RD Nottingham, UK
[b] Laboratoire des Systèmes Perceptifs, École Normale Supérieure, PSL University, CNRS, Paris, France
[c] School of Optometry and Vision Sciences, Cardiff University, CF24 4HQ Cardiff, UK

A B S T R A C T

Topographic maps early in visual processing preserve the spatial relations of visual stimuli but the metric relationships between these visual directions is not directly accessible. To investigate the magnocellular pathway's role in metric spatial vision, we employed an adaptation paradigm. Exposure to a 60 Hz flickering disc array (subjectively invisible) induced a systematic compression in the perceived distance between subsequently presented dot pairs. This compression was strongest when adaptation preferentially modulated low spatial frequency channels, consistent with the properties of transient channels tuned to low spatial and high temporal frequencies. Crucially, this compression was attenuated when the adaptor consisted of two cyan lattices rotating on a magenta background near isoluminance, as confirmed by a global motion direction discrimination task. The same pattern emerged when test dots were isoluminant with the background, ruling out test-adaptor similarity as a critical factor. Finally, an isoluminant red-green adaptor flickering on a yellow background induced compression at 3 Hz, but not at 60 Hz. This dissociation aligns with the known properties of magnocellular neurons, which are insesitive to high temporal frequency isoluminant red-green modulation, but can respond to slow isoluminant red-green modulations. These findings reveal a novel role of the magnocellular pathway in metric spatial vision.

1. Introduction

Topographic maps in the eye and brain maintain the relationships between stimuli in the outside world. However, the metric, or distance, relations between stimuli, cannot be determined by a direct read-out of activity early in the visual processing pipeline, indicating these properties need to be computed in some way. The existence of geometric illusions suggests that spatial computations can be influenced by a variety of factors, including the spatial and temporal proximity of other spatial forms. Apparent distances and directions are subject to perceptual error for specific configurations of spatial form (Robinson, 1972) and figural adaptation can also lead to changes in apparent geometry or scale (Blakemore & Sutton, 1969; Köhler & Wallach, 1944). Typically, figural adaptation leads to a repulsion away from an adaptor within some domain-specific parameter space: a subsequently viewed straight line will appear to have an opposite curvature to a curved adaptor (Gibson, 1933) and a square will appear to be smaller after adapting to a larger square (Köhler & Wallach, 1944). Recently, Hisakata et al. (Hisakata et al., 2016) showed that the distance between two points and the apparent size of a circle can appear compressed after adapting to an array of dots whose positions were updated every 300 ms, even when figural aftereffects were balanced by placing a black square around the adapted (dot array) and the unadapted comparison (grey background field) visual field locations. In this case adaptation in one domain – dot texture, alters perception in another domain – distance, therefore the aftereffect cannot be explained by a within-domain adaptive process. Since the stimulus locations of the comparison patterns were not subjected to adaptation, the change in appearance was attributed to a change in a local metric underlying the representation of visual space. The apparent spatial compression is narrowly tuned to the adapted location and is primarily retinotopic (Jovanovic et al., 2022), suggesting it may be driven by changes early in visual processing.

What classes of cells are being adapted during spatial compression? A major division in the retinocortical pathway is evident in the Lateral Geniculate Nucleus (LGN) (Edwards et al., 2021; Merigan & Maunsell, 1993). Neurons in parvocellular layers are typically colour selective, prefer lower temporal frequencies and can encode fine detail, due to their small receptive fields and dense spatial sampling. The magnocellular layers contain neurons which typically do not respond well to isoluminant colour contrast and are more responsive at low spatial and

☆ This article is part of a special issue entitled: 'Visual Aftereffects' published in Vision Research.

* Corresponding author.
E-mail addresses: lj.m.jovanovic@gmail.com (L. Jovanovic), skoczekkp@cardiff.ac.uk (K. Skoczek), Paul.McGraw@nottingham.ac.uk (P. McGraw), Neil.Roach@nottingham.ac.uk (N. Roach), Alan.Johnston@nottingham.ac.uk (A. Johnston).

https://doi.org/10.1016/j.visres.2025.108680
Received 20 December 2024; Received in revised form 28 July 2025; Accepted 20 August 2025
Available online 27 August 2025

high temporal frequencies. Unlike cells in the parvocellular layer, magnocellular neurons show strong adaptation to contrast, particularly at high temporal frequencies, which is clearly seen after adaptor offset (Solomon et al., 2004; Solomon, 2021). Two spatiotemporal channels have been identified psychophysically that mirror the characteristics of magno and parvo cells. The transient channel responds preferentially to high temporal and low spatial frequencies and sustained channel to low temporal and high spatial frequencies (Anderson & Burr, 1985; Kulikowski & Tolhurst, 1973; Legge, 1978).

Isolating a single cell class or channel in a psychophysical experiment can be challenging (Edwards et al., 2021). Although magno and parvo cells are anatomically separate in the LGN (Merigan & Maunsell, 1993), the information they carry can be combined early in the primary visual cortex (Nealey & Maunsell, 1994; Yoshioka et al., 1994). It is therefore preferable, when trying to target a particular cell type, to focus on the distinguishing properties of LGN cells. The use of high temporal frequencies is helpful in this regard, as retinal and LGN neurons respond to temporal frequencies around 20 Hz higher than cortical cells (Hawken et al., 1996) and magno cells are strongly adapted to contrast at high temporal frequencies but not at low temporal frequencies, providing an opportunity to target the magnocellular pathway through stimulus selection (Solomon et al., 2004). Supporting psychophysical evidence comes from a pulsed pedestal paradigm, suggesting that flicker adaptation desensitises the magnocellular pathway but not the parvocellular pathway (Zhuang et al., 2015). Adaptation at high temporal frequencies, above the critical flicker fusion frequency but within the temporal bandpass of magno cells, can deliver aftereffects even though the adaptor is imperceptible or nearly so (Johnston et al., 2008; Shady et al., 2004; Vul & MacLeod, 2006). In the metric time domain, an apparent duration compression was present at high temporal frequencies (Johnston et al., 2008), which preferentially adapts magno cells and was absent for isoluminant chromatic adaptors, which would not be expected to strongly adapt magno cells (Ayhan et al., 2011).

Here we explore a potential role for magnocellular adaptation in metric spatial vision. To preview our results, we find that adaptation to invisible flicker can induce spatial compression, that spatial compression is stronger for low spatial frequency adaptors and that spatial compression is absent for some isoluminant colour displays.

2. General Methods

Apparatus and stimuli. Stimuli were presented on a Mitsubishi (Chiyoda City, Tokyo, Japan) CRT monitor with refresh rate of 120 Hz, viewed binocularly from a distance of 1 m with a spatial resolution of 1024 x 768 pixels and 1 pixel subtending 1.7 arcmin. A chin rest was used to minimise head movements. Experiments were created using MATLAB R2019 and Psychtoolbox-3 (Brainard, 1997; Kleiner et al., 2007; Pelli 1997), running on a Linux operating system (Ubuntu) and conducted in a dark room. The RStudio environment was used for data analyses. The package"quickpsy" was used for curve fitting, and"r-statix", "ARTool" and "correlation" for statistical analyses (Kassambara, 2019; Kay et al., 2025; Linares & López-Moliner, 2016; Makowski et al., 2020; Wobbrock et al., 2011). The stimuli used to test perceived spatial separation consisted of two pairs of black dots (diameter 0.5 dva). The orientation of the two dots was randomly chosen on each trial and was identical for the two pairs. Adaptors for each experiment are described in specific Method sections.

Observers. Twelve observers participated in Experiment 1 (including four of the authors), eight in Experiment 2 (including two of the authors), seven in Experiment 3A and six in Experiments 3B and 3C (including three of the authors). All observers, except the authors, were naive to the purpose of the experiment and gave an informed consent. The experiment was approved by the University of Nottingham, School of Psychology ethics committee and adhered to the tenets of the Declaration of Helsinki.

3. Experiment 1: Imperceptibly flickering adaptors induce spatial compression

In Experiment 1, we measured the perceived separation of a pair of dots after adapting a region of the vision field to an array of flickering discs. The temporal frequency of the luminance modulation of the uniform black and white discs comprising the adaptor was set to 3 or 60 Hz (with a square-wave modulation). We included a no adaptation baseline condition. The high temporal frequency (60 Hz) adaptor was designed to preferentially adapt transient channels, tuned to high temporal frequencies (Edwards et al., 2021; Kulikowski & Tolhurst, 1973; Solomon et al., 2004). The 3 Hz adaptor was designed to provide evidence of the presence of the standard spatial compression effect for this group of observers. Note, an adaptor consisting of discs flickering between black and white at a temporal frequency of 60 Hz is typically imperceptible, allowing us to investigate whether perceived separation can be biased by adaptation to an invisible adapting field.

3.1. Methods

Stimuli. The adaptor consisted of black (~1cd/m^2) and white (98 cd/m^2) discs, with a diameter 0.5 degree of visual angle (dva) arranged on a regular grid (centre-to-centre separation 1.4 dva), presented within an 11 dva diameter circular aperture. The dot array was presented on a grey background (48.9 cd/m^2). Two pairs of black dots were used to probe the perceived separation. The spatial separation between the two dots in the standard pair was 2 degrees and the separation between the two dots in the comparison paired varied in seven steps, from 0.6 to 1.4 times the standard separation (1.2 – 2.8 dva).

Procedure. Each trial started with a white fixation point presented at the centre of the screen. After 1 s, the adaptor appeared with its onset shaped by a linear ramp. The adaptor was presented for 30 s before the first trial and for a 3 s top-up prior to subsequent trials. The adaptor was centered on an eccentricity of 6 degrees of visual angle on the horizontal meridian, either to the left or to the right of the fixation point. After the adaptor had disappeared, the fixation point changed luminance from white to dark grey for 500 ms, and then to white for 1000 ms, to cue the appearance of the test stimuli. We introduced this delay in order to reduce potential effects of transient attention, and to give observers enough time to prepare for the brief presentation of the test stimuli – two pairs of dots which appeared for 100 ms. Observers were asked to report which pair, presented to the left or to the right of the fixation point, had a greater spatial separation, by pressing a key on a computer keyboard (see Fig. 1A). On half of the trials in each block the standard was presented at the adapted location, and in the other half it was presented at the non-adapted side.

Observers were asked to maintain their gaze at the fixation point in the centre of the screen during the trial. Eye movements were not monitored. The adaptor flickering at 60 Hz was invisible when fixating the centre of the screen, but occasional eye movements made it appear very briefly. To gauge the frequency of these intrusions, we asked observers to press a key to report them on each trial. Observers were informed about this additional task at the beginning the block.

There were three conditions in the experiment: two adaptation conditions and one baseline condition. In the adaptation conditions, the adaptor was flickering (the discs changed luminance polarity) at either 3 or 60 Hz. In the baseline condition no adaptor was presented, but the duration between the trial onset and the onset of the test stimuli was identical to that in the adaptation blocks in order to match the time course of the adaptation conditions. Each condition was presented in a separate block. At the beginning of each block, the block type was clearly indicated to the observers. There were 24 blocks in the experiment, presented in a randomised order (2 adaptor locations (left or right from the fixation point) x 3 conditions (3 Hz, 60 Hz and the baseline) x 4 repetitions). The experiment lasted ~ 4h and was completed over multiple experimental sessions.

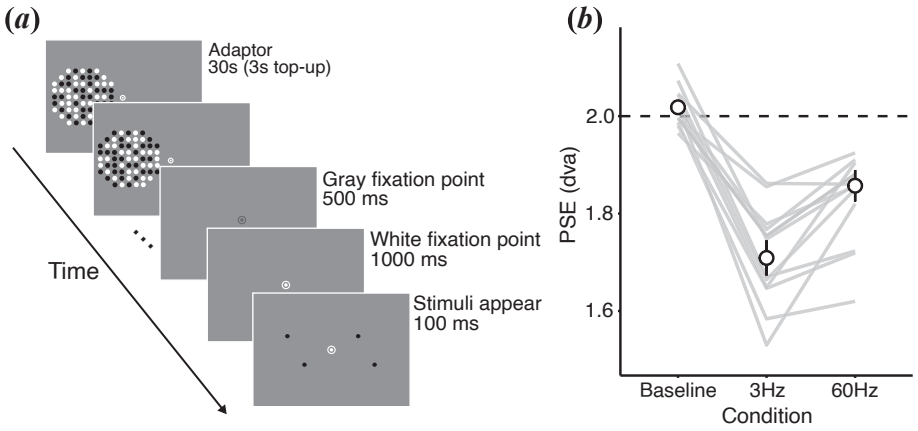

Fig. 1. (a) Schematic representation of adaptation procedure used in Experiment 1. Each trial started with a white fixation point presented at the centre of the screen. Then, an adaptor was presented (30 s in the first trial, three seconds top-up). The adaptor was presented to the left (shown here) or to the right of the fixation point. It consisted of black and white discs changing luminance at a rate of 3 or 60 Hz. After the adaptor disappeared, the fixation point changed luminance to dark grey (500 ms), and then to white (1000 ms). Following this two pairs of dots appeared for 100 ms, to the left or to the right of the fixation point and observers reported which pair had the greater spatial separation. (b) Results of Experiment 1. Median apparent separation compression in the two adaptation (3 and 60 Hz) and baseline conditions. There was a strong compression of the perceived separation after adaptation to discs changing luminance with a frequency of 3 Hz, and smaller but significant effect of the adaptor flickering at 60 Hz. Individual performance is shown with grey lines, and error bars indicate the standard error of median bias in the perceived separation across the observers.

3.2. Results

To quantify the adaptation effects, for each observer in this and subsequent experiments, we calculated the proportion of responses for which the spatial separation between the dots in the comparison pair was considered greater than that of the standard, as a function of the comparison separation. Trials in which the standard dot pair was presented at the same location as the adaptor or on the opposite side of the fixation point were analysed together (after appropriate recoding of responses). We fitted a cumulative normal function to the proportions, to obtain the point of subjective equality (PSE), indicating the physical separation between the dots in the comparison pair judged to be perceptually equivalent to the separation between the dots in the standard pair (Fig. 1b).

As shown in Fig. 1b, adaptation affected the perceived separation in both adaptation conditions, albeit with smaller aftereffects for the 60 Hz adaptor. To quantify these effects, we conducted a Friedman's test, with the PSE as a dependent variable and the adaptation condition (3 Hz, 60 Hz or baseline) as an independent variable. This test confirmed that PSEs are different in the three conditions (χ^2 (2) = 24, $p < 0.01$, effect size W = 1). All three pairwise comparisons were significant (Conover tests, false discovery rate corrected, $p < 0.01$). Next, we checked whether detection of the adaptor due to shifts in gaze during the adaptation phase affected the magnitude of the observed aftereffect. There was large variability between observers with respect to the frequency of adaptor detection (8.6–93 % of trials, median intrusion rate 57 %). To test whether the detection of the adaptor on a given trial caused the compression (for example due to attention directed to the adapted area), we selected only those trials in which no adaptor was reported. For two observers there were fewer than 50 trials in which no adaptor was reported, so their data was excluded from this analysis. A paired Wilcoxon signed rank test revealed that PSEs in the 60 Hz adaptation condition calculated on the subset of trials and observers (median PSE 1.85 (SE = 0.03) vs 1.89 (SE = 0.026) for all observers and trials) was significantly smaller (compression) than the baseline PSE ($p < 0.01$), suggesting that adaptation effects were reliably observed on trials in which adaptor was not detected. Finally, to test whether the observed effect is related to overall exposure to the visible adaptor, we investigated the correlation between the proportion of trials in which the adaptor was reported and the magnitude of the effect and found no evidence for their relationship (Spearman's ρ = -0.006, p = 0.987, and BF01 = 0.617). We found no evidence for a difference in the standard deviations of the cumulative normal distribution (Friedman's test, $\chi 2$ (2) = 0.667, p = 0.717), suggesting that the adaptation did not alter sensitivity of separation judgements.

These results suggest that the spatial compression at high temporal frequency could be due to adaptation of magno cells or their retinal precursors (Solomon et al., 2004). In addition, we can discount parallels with classical figural aftereffects here since the shape of the adaptor array was invisible (Köhler and Wallach, 1944). There is a clear compression of visual space after 3 Hz adaptation replicating previous work (Hisakata et al., 2016; Jovanovic et al., 2022). The stronger effect in the case of the 3 Hz adaptor suggests the strength of the adaptation may be tuned to temporal frequency. Stronger adaptation in the case of the 3 Hz adaptor could result from adaptation of other cell types, such as parvo cells, which respond well to 3 Hz stimulation (Derrington & Lennie, 1984), although the fact that magno cells are more likely to show effects of adaptation supports magnocellular involvement (Daumail et al., 2023; Raghavan et al., 2023; Solomon et al., 2004).

4. Experiment 2: Low spatial frequency content is responsible for the spatial compression

Results of Experiment 1 are consistent with the hypothesis that the activity of transient channels may be responsible for the adaptation-induced spatial compression. There are at least two temporal channels, tuned to low and high temporal frequencies (Hammett & Smith, 1992; Johnston & Clifford, 1995; Mandler & Makous, 1984). Transient channels are more sensitive at low spatial frequencies and sustained channels are relatively more sensitive at high spatial frequencies (Kulikowski & Tolhurst, 1973). Here we test the dependency of spatial compression on the spatiotemporal frequencies of the adapting stimulus using Gabor array adaptors.

4.1. Methods

Stimuli The adaptor consisted of Gabor patches displayed on a mid-grey background (48.9 cd/m^2). The Gabor patches consisted of a sine grating drifting inside a static Gaussian envelope (standard deviation 0.17 dva, temporal frequency 3 or 10 Hz). The spatial frequency of the grating carrier was 0.5, 2, 5, 10 or 15 cpd, with contrast set at 90 % prior to windowing and with orientations randomly chosen for each patch on

each trial. The adaptor array consisted of 45 patches presented within a circular region of 10 dva diameter, with centre-to-centre separation between patches of 1.25 dva (Fig. 2). The spatial separation between the two dots in the standard pair was 1 degree and the separation between the two dots in the comparison pair varied in seven steps, from 0.6 to 1.4 of the standard separation.

Procedure. The procedure was the same as in Experiment 1, except that the adaptor was presented for 60 s in the first trial of a block (5 s top-up), and the standard dot pair was always presented at the adapted location. There were 20 blocks in the experiment presented in a randomised order (2 adaptor locations (left or right from the fixation point) x 2 temporal frequencies (3 Hz or 10 Hz) x 5 spatial frequencies (0.5, 2, 5, 10 and 15 cpd)). The experiment lasted ~ 3 h and was completed across multiple experimental sessions.

4.2. Results

The point of subjective equality as a measure of the perceived separation is shown in Fig. 2b, for different the spatial and temporal frequencies of the adaptor (colour coded).

A repeated measures ANOVA with aligned rank transformed data (Wobbrock et al., 2011) (F tests with Kenward-Roger degrees of freedom), with the PSE as a dependent variable, and the temporal and spatial frequency as independent variables, indicated there was an effect of spatial frequency (Wald F (4, 63) = 29, $p < 0.01$, $\eta^2 = 0.65$), but no effect of temporal frequency (Wald F (1, 63) = 0.31, p = 0.57) and no interaction (Wald F (4, 63) = 2.26, p = 0.073). Pairwise comparisons (fdr corrected) showed that when adaptor Gabor patches drifted at 3 Hz there was a significant difference in PSEs between 15 and 0.5, 2 and 5 cpd conditions. When Gabor patches drifted at 10 Hz, there was a significant difference between 0.5 and 2, 10 and 15 cpd conditions, between 2 and 10 cpd conditions, as well as a significant difference between 5 and 15 cpd conditions. When compared to the baseline performance, Wilcoxon signed-rank tests (fdr corrected) indicated that there was a significant bias induced by the adaptation in all conditions except for the adaptor consisting of Gabor patches with a spatial frequency 15 cpd (in both temporal frequency conditions). As in Experiment 1, we found no evidence for an effect of spatial frequency (Wald F (4, 63) = 0.986, p = 0.427), temporal frequency (Wald F (1, 63) = 1.652, p = 0.203) or their interaction (Wald F (4, 63) = 0.318, p = 0.865) on the sensitivity as indicated by the slope of the psychometric function.

The observation of the greater effect for low spatial frequency Gabor patches is consistent with a bias towards magnocellular processing at low spatial frequency (Edwards et al., 2021). Although there is considerable overlap in the spatial frequency tuning of parvocellular and magnocellular neurons there is a bias towards greater sensitivity of magno cells at low spatial frequencies and towards greater sensitivity of parvo cells at high spatial frequencies (Derrington & Lennie, 1984). Lesion studies show a greater loss of contrast sensitivity at low spatial frequencies and higher temporal frequencies after magnocellular layer LGN lesions and a greater loss of contrast sensitivity at high spatial and low temporal frequencies after parvocellular layer lesions (Merigan & Maunsell, 1993). The greater spatial compression effect for low spatial frequency Gabor patches and the lack of evidence for an effect of temporal frequency found here is consistent with the view that the spatial compression effect is primarily driven by magnocellular adaptation.

5. Experiment 3A: The luminance signal in colour adaptors modulates the magnitude of spatial compression

The results so far implicate transient channels tuned to low spatial and high temporal frequency modulation in the perception of the spatial separation adaptation effect. Considerable evidence suggests that luminance and chromatic signals are processed differently in the segregated layers of the LGN (De Valois, Abramov, & Jacobs, 1966; Kaiser, Lee, Martin, & Valberg, 1990; Lee, Martin, & Valberg, 1988; Lee, Pokorny, Smith, Martin, & Valbergt, 1990; Schiller & Colby, 1983). The parvocellular system consists of cells whose receptive field centre and surround are preferentially sensitive to a different range of wavelengths, making them selective for both chromatic and luminance contrast. Magnocellular neurons on the other hand receive approximately equal inputs from different wavelength signals in both centre and surround and have little sensitivity to colour, although there is evidence for some overlap between luminance and colour sensitivities in the two pathways (Gouras & Zrenner, 1979; Lee & Sun, 2009). Presentation of an isoluminant chromatic adapting field should allow us to isolate the specific

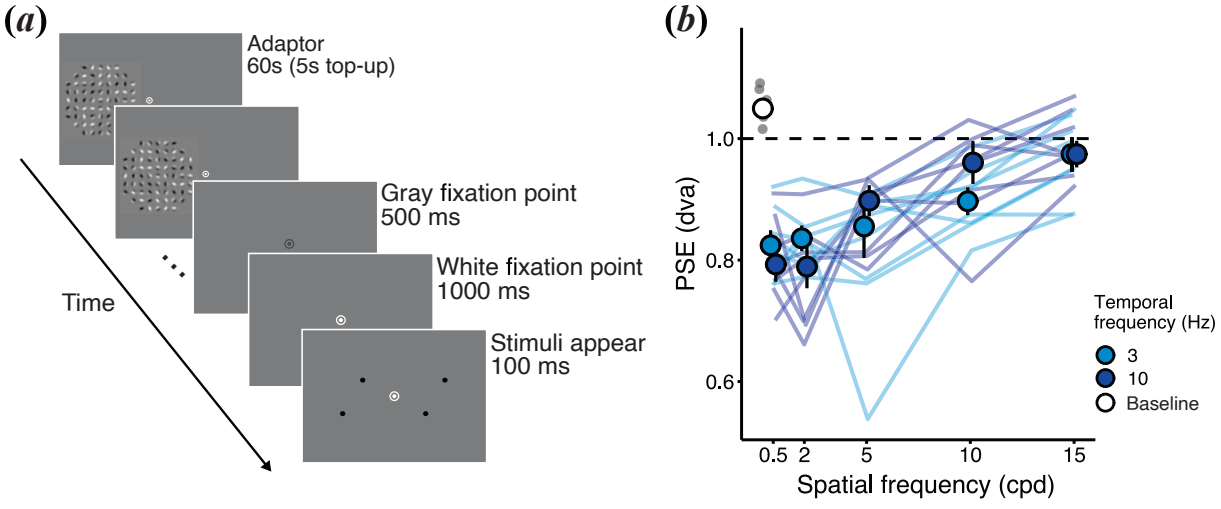

Fig. 2. (a) Schematic representation of the procedure for Experiment 2. On each trial, an adaptor composed of an array of Gabor patches was presented (60 s in the first trial, five seconds top-up), to the left (shown here) or to the right of the fixation point. The spatial and temporal frequencies of the Gabor patches were varied across blocks. After the adaptor had disappeared and following a change in luminance of the fixation point, two pairs of dots appeared for 100 ms, to the left or to the right of the fixation point. Observers reported which pair had a greater spatial separation. (b) Results of Experiment 2. Median apparent separation compression is shown for the five spatial frequencies and the baseline (white symbol), separately for adaptor arrays drifting with temporal frequencies of 3 and 10 Hz (blue and cyan symbols, respectively). The apparent compression was greatest for adaptors with spatial frequencies smaller than 5 cpd, irrespective of the temporal frequency of the drift. Median apparent separation compression is shown with dots, and individual performance is shown as lines. Error bars indicate standard error of median across observers. (For interpretation of the references to colour in this figure legend, the reader is referred to the web version of this article.)

contribution of the luminance signal in adaptation-based spatial separation compression. To reduce dependence on the linear temporal summation of dynamic chromatic signals, we used motion rather than a flicker for our isoluminant adaptor, and we used just one colour (cyan) for the moving dots which were presented on a magenta background. We set the colours of the foreground dots and background to lie close to the M−L axis of DKL space (Derrington et al., 1984) and then we "bracket" the isoluminant point by varying the luminance difference between the foreground stimulus and background. We also established an independent estimate of the isoluminant point for each observer, by measuring the point of breakdown of global motion grouping at isoluminance using the same stimulus (Johnston et al., 1999; Livingstone & Hubel, 1987).

5.1. Methods

Stimuli and apparatus were identical to those in previous experiments, but with a different adaptor stimulus. In this experiment, the adaptor pattern was made up of two grids of cyan dots (CIE xyY [0.240, 0.333, varying luminance]) presented on a magenta background (CIE xyY [0.317, 0.304, 31.7]). The colours were chosen to isolate the L-M colour opponent mechanism. The luminance of the adapting dots was kept constant within a block, at one of 9 levels per block: 5, 10, 16.2, 26.2, 30.2, 32.7, 40.4, 43.6 or 55.4 cd/m^2, measured with a ColorCal MkII colorimeter (CRS Ltd, Kent, UK). Each dot was 0.33 degrees of visual angle in diameter and moved along a square path with side length 0.8 degrees of visual angle at a speed of 4 degrees per second. The grids were positioned such that dots appear in pairs occupying opposite points along the perimeters of the square motion path (Fig. 3). The adaptor pattern spanned 6 degrees of visual angle vertically and horizontally, centred at a point 11 degrees of visual angle either to the left or right of fixation point. A baseline condition was also tested where no adaptor was presented.

Procedure. The psychophysical task was the same as in previous experiments: observers viewed an adapting pattern (for 30 s on the first trial, followed by 3 s top-ups between trials), and reported which of two pairs of test dots appeared to have the greatest separation. The separation of the standard pair of dots was kept constant (2 dva) while the separation of the comparison pair at each trial was determined by a QUEST algorithm (Watson & Pelli, 1983) set to converge to 50 % correct performance. Two QUEST algorithms were used concurrently within each block, corresponding to whether the standard or comparison pair of dots were presented at the adapted location on a particular trial. After completing the collection of the adaptation data, a second task was carried out to explore the visibility of the adaptor pattern. Observers viewed an adaptor pattern and were asked to report on which side the adaptor dots were presented (two-alternative forced choice (2AFC), left or right) and the direction of motion (clockwise or anticlockwise). Each adaptor luminance level was presented 80 times, an equal number of times to the right or left of fixation and an equal number of times with each direction of motion.

5.2. Results

Observers' responses were combined across visual field locations and used to generate two values of the PSE (taken as the QUEST 50 % threshold estimate) per luminance level for each observer, corresponding to whether the standard or comparison dot pair were presented in

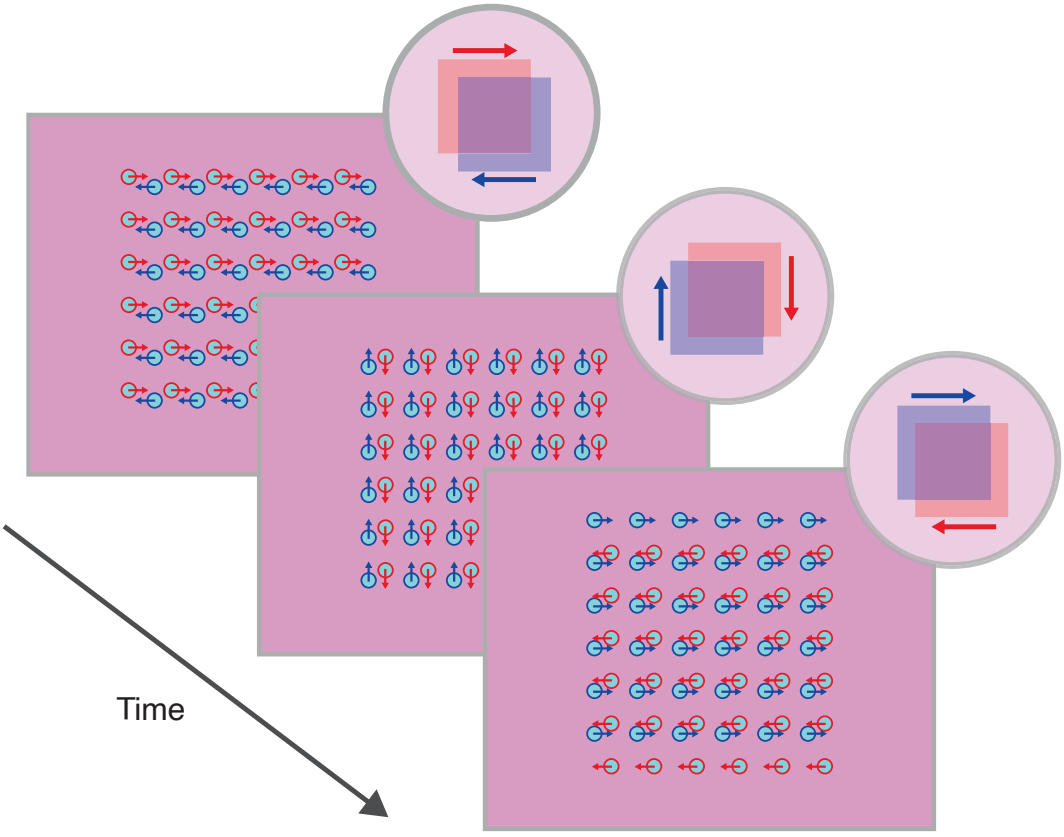

Fig. 3. Schematic representation of adaptor used in Experiment 3A. The adaptor pattern was made up of two grids of cyan dots (red and blue outline of dots displayed here is only for illustration purposes), presented on a magenta background, to isolate the L-M colour opponent mechanism. Each dot moved along a square path with side length 0.8 degrees of visual angle at a speed of 4 dva per second, for 30 s (3 s top-up). Luminance of dots was varied in different blocks, to test whether the adaptation-induced spatial compression depends on the luminance difference between the adaptor and the background. (For interpretation of the references to colour in this figure legend, the reader is referred to the web version of this article.)

the adapted field location (32 trials per estimate). The magnitude of compression was calculated as the difference between the QUEST threshold estimates for the adapted and baseline condition, transformed such that positive differences indicated the presence of compression. These magnitude values were then averaged between standard and comparison dot pair adaptation conditions for each observer and luminance level. Finally, magnitude values were normalised across observers by dividing each magnitude value by the average of each observer's compression magnitudes observed with the brightest and darkest adaptor dots (i.e. the greatest contrast, where compression was observed to be strongest).

Normalised measures of compression magnitude as a function of relative luminance (difference between the background and luminance of the adaptor) are shown in Fig. 4a. When the adaptor dots were closest in luminance to the background (i.e., near isoluminance), the compression aftereffect was reduced in magnitude. A Friedman's test indicated a significant difference in compression magnitude between levels of dot luminance (χ^2 (8) = 23.3, $p < 0.001$, effect size W = 0.485). Pairwise-comparisons (Conover test with fdr correction) indicated that adapting dots that were closest in luminance to the background (+0.91 cd/m^2) produced significantly less compression ($p < 0.05$) than all other luminance levels, except the second closest (−1.47 cd/m^2). Significant differences were also found between adaptation to a −1.47 cd/m^2 adaptor and those at two other luminance levels (−26.7, −21.65 cd/m^2, $p < 0.05$), as well as between 11.93 and −21.65 cd/m^2. To obtain estimates of sensitivity, we binned the presented test separations in five equally-sized bins (~26 trials in a bin, binning was done separately for each observer and condition). Then, for each observer and condition we fitted data with a cumulative normal distribution to obtain estimates of its PSE and standard deviation. As before, we found no evidence for a difference in standard deviations of the cumulative normal distribution (χ^2 (8) = 7.56, p = 0.478).

At isoluminance the global motion of the dots becomes completely disorganized (Johnston et al., 1999; Livingstone & Hubel, 1987). When asked to report whether the adaptor dots moved clockwise or anti-clockwise, observers achieved > 90 % performance at all luminance levels except + 0.91 cd/m^2, where median performance fell to 66 % (range 51 % − 70 %). This reduced performance appears much more tightly tuned to physical isoluminance than the magnitude of the compression effect (Fig. 4c). However, while observer's ability to determine the direction of motion in the adaptor dots was severely reduced near isoluminance, the adaptors were never rendered undetectable, and accuracy in reporting the location of the dots did not fall below 95 % for any observer at any luminance level (Fig. 4b).

Although the adaptor was always visible, even near isoluminance, global motion perception broke down close to isoluminance, presumably due to a breakdown in local motion computation caused by a loss of magnocellular pathway signal strength. At that adaptor's relative luminance level there was also a clear reduction in the apparent spatial compression effect, directly linking the spatial compression effect to an impoverished magnocellular signal.

6. Experiment 3B: The luminance signal in colour adaptors modulates the magnitude of spatial compression for isoluminant test dots

Evidence presented thus far suggests a dominant role for luminance information in adaptation-induced spatial separation compression. However, so far we have only tested separation compression with luminance-defined dot pairs. Previous work showed that separation compression can be induced by different adaptors (sine gratings, Gabor arrays, updating dot arrays with or without positional jitter or motion; Hisakata et al., 2016; Hisakata & Kaneko, 2021; Jovanovic et al., 2022), suggesting that direct correspondence between adaptor and test patterns may not be necessary. That said, adaptation-induced biases in perceived spatial location of visual stimuli have been shown to depend on whether the adaptor and test patterns lie along the same cardinal axis in colour space (McGraw et al., 2004). To directly address the question of specificity of adaptation to luminance defined-stimuli, we tested a subset of conditions from Experiment 3A, using test dot pairs that matched the adaptor in colour (magenta) and were isoluminant with the background. This manipulation allowed us to test the specificity of the adaptation

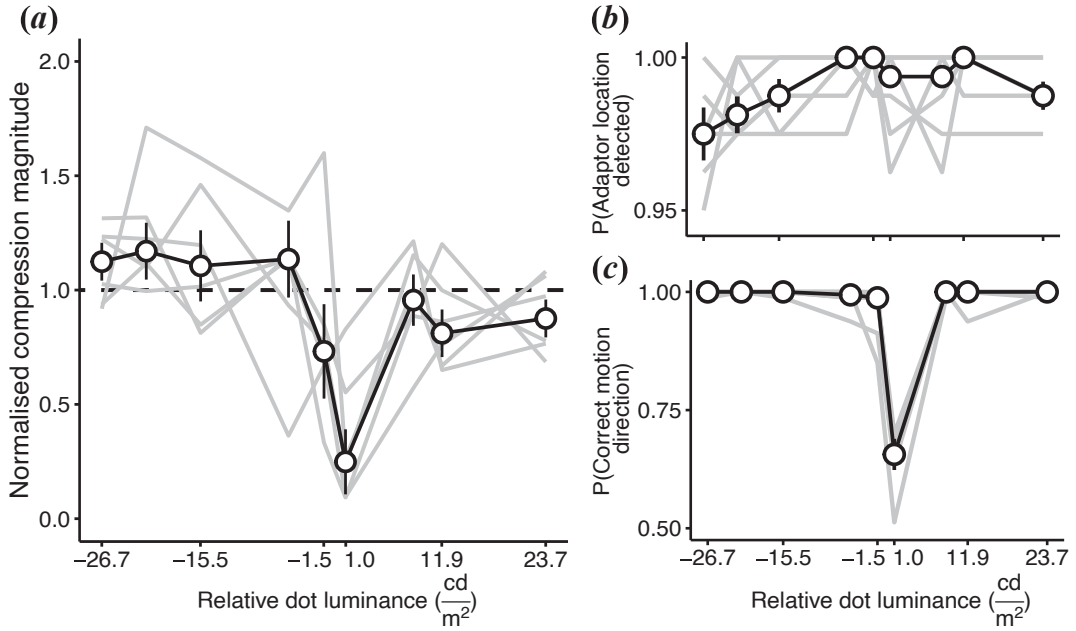

Fig. 4. (*a*) Results of Experiment 3A. Magnitude of normalised compression in perceived separation as a function of the luminance of the adaptor dots (relative to background luminance). A significant reduction in compression magnitude was found when adaptor dots were close to isoluminant with the background, compared to when greater luminance contrast was present. Individual performance is shown in grey lines, and error bars indicate the standard error of the median across the observers. (*b*) Results of the dot detection task. Observers were consistently able to report correctly the location of presented dots with above 95% accuracy across all levels of dot luminance. (*c*) Results of the dot motion direction task. A sharp reduction in accuracy in reporting the direction of dot motion occurred at luminance contrast closed to isoluminance, coinciding with reduced compression magnitude seen in panel *a*.

mechanism.

6.1. Methods

Stimuli and apparatus were identical to those in Experiment 3A, with a few modifications. In this experiment, three adaptor conditions were tested, in which luminance of cyan dots forming the adaptor was either 5, 30 or 55 cd/m^2 (CIE xyY [0.240, 0.333, varying luminance]). The dot pairs used to test separation discrimination were isoluminant with the background (CIE xyY [0.240, 0.333, 30]), and measured 0.34 degrees of visual angle in diameter. The duration of the test dots was increased to 300 ms. For one observer who had difficulty perceiving the isoluminant test dots, the duration was increased to 500 ms. A baseline condition (no adaptor) was also tested. The viewing distance was 57 cm.

Procedure. The psychophysical task was identical to that in Experiment 3A. Each adaptor luminance level was presented 80 times, an equal number of times to the right or left of fixation point and equally across both motion directions.

6.2. Results

Observers' responses were analysed in the same way as in Experiment 3A. Normalised measures of compression magnitude as a function of relative luminance (the difference between the background and adaptor luminance) are shown in Fig. 5. We replicated the general pattern found in Experiment 3A: there was an adaptation effect in conditions with large luminance difference between the adaptor dots and the background. This compression effect was reduced when the adaptor and the background had the same physical luminance.

A Friedman's test indicated a significant difference in compression magnitude between levels of dot luminance (χ^2 (2) = 9.33, $p < 0.01$, effect size W = 0.778). The same outcome was obtained after exclusion of the observer for whom test dots were presented for 500 ms (χ^2 (2) = 8.4, $p < 0.05$, effect size W = 0.840). Pairwise-comparisons (Conover test with fdr correction) indicated that adapting dots that were isoluminant with the background produced significantly less separation compression ($p < 0.01$) compared to the other two conditions. Furthermore, there was no evidence for a difference in the separation compression between the two conditions in which adapting dots were luminance-defined (−25 vs + 25 cd/m^2 relative to the background luminance, $p = 0.230$). As before, we found no evidence for a difference in the standard deviations of the cumulative normal distribution (χ^2 (2) = 4.33, p = 0.115). Of note, standard deviations were twice the magnitude of those found in Experiment 3A, suggesting that the task was more difficult with isoluminant stimuli even though they were presented for longer time (~0.5 dva in Experiment 3A and ~ 1 dva in Experiment 3B).

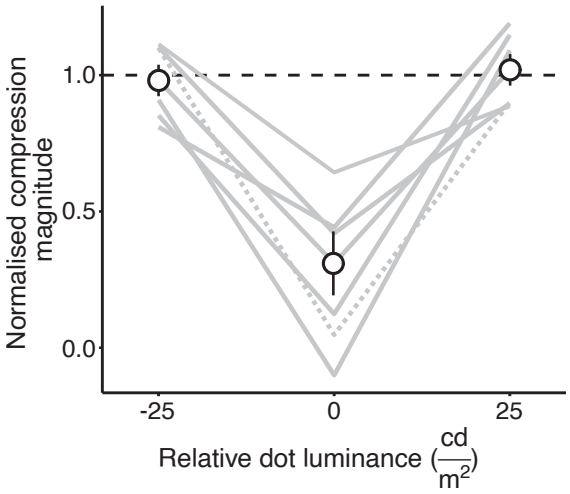

Fig. 5. Results of Experiment 3B. Normalised magnitude of compression in perceived separation as a function of the luminance of the adaptor dots (relative to the background luminance). A reduction in compression magnitude was found when the adaptor dots were close to isoluminant with the background, compared to conditions with greater luminance contrast. Individual performance is shown by grey lines, and the dashed line indicates performance for one observer for whom separation discrimination was measured with test dots presented for 500 ms. Error bars indicate the standard error of the median across the observers.

In summary, sensitivity in the separation discrimination task with test stimuli isoluminant with the background was lower (Kelly, 1983; Lambert et al., 2003; Webster et al., 1990). Nevertheless, we found evidence for adaptation-induced spatial distance compression, that was diminished at physical isoluminance between the adaptor and background, as was the case for the luminance-defined test stimuli in Experiment 3A.

7. Experiment 3C: Isoluminant red-green modulation induces spatial compression

There are a number of reports that non-human primate LGN magno cells are responsive to isoluminant red-green flicker (Kaiser et al., 1990; Lee & Sun, 2009; Schiller & Colby, 1983). In particular, stimulating with isoluminant red-green flicker produces a frequency doubled response that falls off above approximately 20 Hz (Lee et al., 1990) and would therefore have no influence at 60 Hz. As a further test of the magnocellular adaptation hypothesis we replicated Experiment 1 replacing luminance modulation with isoluminant red-green modulation.

7.1. Methods

Stimuli and procedure were identical to those of Experiment 1. The only difference was the colour and luminance of the discs comprising the adaptor and the background. The discs changed colour from red (CIE xyY [0.61 0.34 22.7]) to green (CIE xyY [0.3 0.58 22.7]) and were presented on a yellow background (CIE xyY [0.49 0.43 23]). Additionally, discs were smoothed (standard deviation of 0.5 dva). Since the adaptor was large and spanned a range of eccentricities, a pilot experiment showed that it was very difficult to use matching techniques to obtain subjective isoluminance (Anstis & Cavanagh, 1983; Edwards, Goodhew, & Badcock, 2021), and we opted to present physically isoluminant adaptors to all observers. Chromatic flicker above 25 Hz is likely too fast to be resolved by the human visual system (Lee et al., 1990; Jiang et al., 2007). However, we included the 60 Hz condition as a control to test whether residual luminance signals were present and sufficient to induce adaptation (Lee et al., 1990). In this condition, the chromatic adaptor was detected on average on 1.1 % of trials (0–8.7 %), suggesting that it was processed by the slow chromatic pathway. All seven observers also took part in Experiment 1, which allowed for a within-individual comparison of adaptation effects.

7.2. Results

The point of subjective equality for each observer (gray lines, medians shown with white symbols) and the three conditions are shown in Fig. 6a. A Friedman's test showed that there was an effect of condition on PSEs (χ^2 (2) = 11.1, p < 0.01, effect size W = 0.796). Pairwise comparisons indicated that the perceived separation was reduced following adaptation to an adaptor changing colour with a frequency of 3 Hz relative to both the baseline and 60 Hz condition (Conover's test, p < 0.01, fdr corrected). As expected, there was no difference between the baseline and 60 Hz condition. There was no evidence for an effect of adaptation on the sensitivity of separation judgements (χ^2 (2) = 1.14, p = 0.565). To directly test the effect of the luminance signal, we compared the adaptation effects for the colour (Experiment 3C) and luminance-modulated (using a subset of observers from Experiment 1)

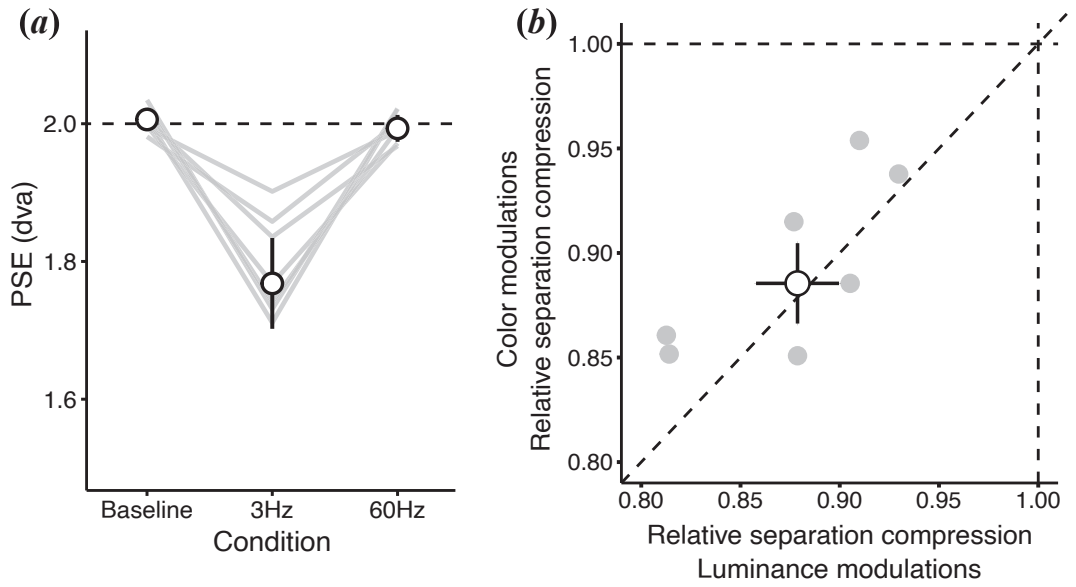

Fig. 6. (a) Results of Experiment 3C. Median apparent separation compression in the two adaptation (red-green modulations with frequency of 3 and 60 Hz) and the baseline conditions. There was a strong compression of the perceived separation after adaptation to red and green discs changing colour with a frequency of 3 Hz, and no effect of the 60 Hz modulations. Individual performance is shown in grey lines, and error bars indicate the standard error of median bias across the observers. (b) Comparison of relative separation compression following exposure to isoluminant colour modulations (Experiment 3C) and luminance modulations (Experiment 1). There was no evidence for a difference in the relative compression for the two adaptor types. Median relative compression is shown with white, and individual performance is shown with grey symbols. Error bars indicate standard error of median across observers.

adaptor in the 3 Hz condition. We compared the relative compression aftereffect (Fig. 6b), by dividing the PSEs in the 3 Hz condition by the baseline performance, to account for minor differences between the two experiments (e.g. different colour and luminance of the background). As shown in Fig. 6b, there was no evidence for a difference in the relative compression induced by temporal modulations of colour and luminance (Wilcoxon signed rank test, $p = 0.1563$, $BF01 = 11.65$).

In Experiment 3C there was no evidence for an effect of chromatic flicker at 60 Hz, although we did see a compression after 60 Hz luminance flicker in Experiment 1. We can conclude from these results that the spatial compression effect can be induced by magno cells (Experiment 1) and that, as expected, when the stimulus was defined by high frequency chromatic flicker, neither the magnocellular nor parvocellular cells would be activated (Experiment 3C). However, we also found a spatial compression effect following adaptation to the 3 Hz isoluminant adaptor. The similarity to the aftereffects caused by the 3 Hz luminance flicker could result from the fact that 3 Hz isoluminant red-green flicker may stimulate the magnocellular pathway, in agreement with a number of observations that monkey LGN magno cells are responsive to isoluminant red-green flicker (Kaiser et al., 1990; Lee & Sun, 2009; Schiller & Colby, 1983). Isoluminant red-green flicker produces a frequency doubled response that falls off above approximately 20 Hz (Schiller & Colby, 1983) and would clearly have no influence at 60 Hz. There is also a first-harmonic response in magno cells at lower temporal frequencies (Lee & Sun, 2009). Of note, our choice of using physical isoluminance for the adaptor design could potentially introduce a heterogeneity in responses to the flicker across observers. However, if there was some marginal stimulation of a luminance-based mechanism this was not sufficient in magnitude to generate spatial compression at 60 Hz.

8. Discussion

We found that exposure to an array of discs flickering from black to white at a frequency of 60 Hz caused a significant compression of the perceived distance between two subsequently presented dots, albeit to a somewhat lesser degree than for a lower temporal frequency (3 Hz) adaptor. The spatiotemporal profile of the adaptor suggests involvement of spatially low-pass, temporally band-pass transient channels in spatial compression. This hypothesis is supported by results of Experiment 2, showing that the magnitude of compression depends on the spatial frequency of adaptors: there was a strong compression of perceived separation with low but not high spatial frequency adaptors.

Previous work found that a dynamic adaptor (lattice of dots changing luminance and position) leads to a greater reduction of apparent object size than a static adaptor (Hisakata & Kaneko, 2021), suggesting that both the spatial properties of the adaptor and its temporal dynamics are involved in generating the aftereffect. The presence of a compression effect with invisible adaptors demonstrates that the current finding can be distinguished from classical figural aftereffects (Hisakata et al., 2016; Köhler & Wallach, 1944) and is unlikely to be caused by attentional effects associated with the adaptor, although attention may nevertheless enhance adaptation when the adaptor is clearly visible (Hisakata & Kaneko, 2021; Yeh et al., 1996). Small fixational eye movements caused the high temporal frequency adaptor to be visible for very brief periods. However, the frequency of these intrusions was not related to the magnitude of the aftereffect, and excluding trials where intrusions were reported did not change the magnitude of the observed effects. This dissociation suggests that conscious perception of the spatial properties of the adaptor was not required to modify the mechanism encoding spatial relations between objects (Blake & Fox, 1974; Smith & Henriksson, 1955; Tagoh et al., 2022). That said, the stronger aftereffect for the 3 Hz adaptor observed in Experiment 1 suggests some degree of temporal frequency tuning in the strength of adaptation.

The high temporal frequency adaptor was chosen to target the magnocellular pathway. Magno cells in the LGN respond to higher temporal frequencies than parvo cells and cells in primary visual cortex. In addition, magno cells show stronger adaptation than parvo cells, with adaptation potentially being inherited from retinal precursors (Camp, Tailby, & Solomon, 2009; Daumail et al., 2023; Raghavan et al., 2023; Solomon, Peirce, Dhruv, & Lennie, 2004; Tailby et al., 2007; Zhuang, Pokorny, & Cao, 2015) and electrophysiological evidence in non-human primates suggests that, although all cell types in the lateral geniculate nucleus adapt to a 4 Hz, 1 cpd drifting grating, only magnocellular

neurons show adaptation in the averaged, population response (Daumail et al., 2023). The high frequency adaptor was imperceptible, but we do not wish to suggest that this means there is no cortical activation or no consequence of sub-cortical adaptation for cortical processing. There is evidence from fMRI that invisible chromatic flicker can give rise to cortical activation (Jiang et al., 2007), however we should note that fMRI extracts signals present in the brain by averaging blood flow over seconds and it is not clear that these signals are functional on physiological time scales or sufficient to give rise to conscious experience. A similar argument applies to observations about neural temporal synchrony at imperceptibly high flicker rates, as neural spike timing observed externally is not necessarily linked to visual experience or information processing within neural systems. However, orientation selectivity is a key feature of cortical processing, and orientation specific contrast adaptation to high flicker rate invisible grating adaptors has been observed (Falconbridge et al., 2010), clearly implicating cortical involvement in high frequency flicker adaptation.

Given that magno cells are less sensitive to chromatic contrast than parvo cells, we investigated the magnitude of the spatial compression effect using physically isoluminant adaptors in two complementary paradigms. In an effort to silence the magnocellular response and simultaneously approximate the optimal isoluminant point, we used an adaptor that consisted of two rotating dot latices, which appeared as two rotating sheets when there was a luminance difference between the dots and background and as randomly moving dots at isoluminance. The dot and background colours were chosen to lie close to the L-M axis of DKL space. The spatial compression effect was virtually eliminated close to the isoluminance point as indicated by a perceptual loss of global motion structure. The co-occurrence of the lack of global motion organization with the loss of spatial compression at isoluminance provides strong evidence for magnocellular involvement in the spatial compression effect. We repeated the experiment with a subset of luminance difference levels between the adapting dots and the background, but with test dots isoluminant with the background. We observed the same pattern of results, indicating that the effect depends upon the nature of the adaptor and not on the visual properties used to specify the test intervals. In the second approach, the adaptor consisted of an array of dots flickering between red and green on a yellow background. This induced a subsequent spatial compression at low but not at high temporal frequencies. The high temporal frequency result is consistent with a lack of magnocellular response to chromatic modulation and a lack of parvocellular activation at high temporal frequencies. The presence of spatial compression after low temporal frequency adaptation is consistent with reports of magnocellular sensitivity to isoluminant red-green modulation at low temporal frequencies (Kaiser et al., 1990; Lee & Sun, 2009; Schiller & Colby, 1983).

The strategy of using a stimulus to selectively activate neural populations tuned to that stimulus and observing the effect of neuronal adaptation of subsequent visual processing has proven to be a very effective means of targeting and isolating visual mechanisms. In the case of the spatial compression effect, it has been demonstrated for adaptors that are varied in nature (e.g. sine gratings, Gabor arrays, updating dot arrays or rotating dot arrays) and very different from the test patterns (e.g. pairs of isolated dots or circles, Hisakata et al., 2016; Hisakata & Kaneko, 2021; Jovanovic et al., 2022). There is no requirement for the close correspondence between adaptor and test that is typical of feature specific adaptation, such as orientation specific contrast adaptation for sine wave gratings (e.g. Dao et al., 2006). Here we report that the adaptatison-based spatial separation compression occurs for both luminance and colour-defined test stimuli (when adaptor is luminance-defined), complimenting previous findings (see also McKeefry et al., 2006). These converging findings suggest that adaptation is has a more general effect, beyond simply reducing the sensitivity of the visual system to the adapting stimulus.

Since the separation of the test dots appears to change, although their locations in the image, in the retina and in cortical maps do not, it has been proposed that computing separation involves an explicit neural representation of local scale, as well as a control process integrating signals reflecting units of that metric across the space, the fundamental unit of distance computation (Hisakata et al., 2016). There is some evidence suggesting that the metric and the control process can be dissociated (Hisakata & Kaneko, 2021). That the system can be adapted implies that the metric is computed from the image, and the compression implies that adaptation reduces the value of the metric in an analogous way to the reductions seen in perceived contrast or perceived speed after adaptation to those visual properties.

It has been proposed that adaptation-induced spatial compression might be a consequence of adaptation to global borders of the adaptor (Zimmermann, 2023). It has been shown that adaptation to a spatially localised adaptor provokes a compression of perceived distance between two dots presented within the adapted region, but an expansion when the dots straddle the adapted region. To account for both of these effects, it was proposed adaptation to the adaptor border might depress neuronal firing locally, leading to a compression of space at the adapted position and expansion close the adapted location (border). However, it is still not clear whether these two effects (compression and expansion) come from the same mechanism and paradigms proposed in this manuscript, such as adaptation to an adaptor flickering with suprathreshold frequency, might offer some insight into this question.

The evidence reported above indicates a novel and prominent contribution of the magnocellular pathway in metric spatial vision. There is evidence that some forms of developmental dyslexia are related to a magnocellular deficit (Amitay et al., 2002; Gori et al., 2016; Stein & Walsh, 1997, although see Stein, 2019). However, much of the evidence comes from deficits in temporal or motion processing (Johnston et al., 2008; Gori et al., 2016; Stein & Walsh, 1997), while the difficulty reported in developmental dyslexia, is often characterized as a spatial vision problem, in that letters and words appear poorly formed or in the wrong place. A role for the magnocellular pathway in apparent spatial compression outlined here provides a putative bridge between magnocellular deficits and disordered spatial vision.

In summary, we have provided evidence that adaptation to dynamic pattern can alter the perceived separation of spatial features. The adaptation is greatest for low spatial frequency adapters and can occur at high temporal frequencies for which the adaptor is imperceptible. The apparent spatial compression is eliminated for isoluminant adaptors which also lead to disordered global motion, implicating the magnocellular pathway.

Funding.

This work was supported by the Leverhulme Trust (RPG-2019–309).

Ethics. The experiment was approved by the University of Nottingham, School of Psychology ethics committee and adhered to the tenets of the Declaration of Helsinki.

Use of Artificial Intelligence (AI) and AI-assisted technologies. No AI or AI-assisted technologies were used in this work.

Data, code and materials. Data and code are available at https://osf.io/ewj36/?view_only=4f7d3580b55942818443fa048752a46f.

CRediT authorship contribution statement

Ljubica Jovanovic: Writing – review & editing, Writing – original draft, Software, Methodology, Investigation, Data curation, Conceptualization. **Kristian Skoczek:** Software, Methodology, Investigation, Data curation, Conceptualization. **Paul McGraw:** Writing – review & editing, Methodology, Conceptualization. **Neil Roach:** Writing – review & editing, Methodology, Conceptualization. **Alan Johnston:** Writing – review & editing, Supervision, Methodology, Funding acquisition, Conceptualization.

Declaration of competing interest

The authors declare that they have no known competing financial

interests or personal relationships that could have appeared to influence the work reported in this paper.

Data availability

Link to data is provided in the manuscript

References

Amitay, S., Ben-Yehudah, G., Banai, K., & Ahissar, M. (2002). Disabled readers suffer from visual and auditory impairments but not from a specific magnocellular deficit. *Brain, 125*(10), 2272–2285.

Anderson, S. J., & Burr, D. C. (1985). Spatial and temporal selectivity of the human motion detection system. *Vision Research, 25*(8), 1147–1154.

Anstis, S., & Cavanagh, P. (1983). *A minimum motion technique for judging equiluminance* (pp. 66–77). Toronto: York University.

Ayhan, I., Bruno, A., Nishida, S. Y., & Johnston, A. (2011). Effect of the luminance signal on adaptation-based time compression. *Journal of Vision, 11*(7), 22.

Blake, R., & Fox, R. (1974). Adaptation to invisible gratings and the site of binocular rivalry suppression. *Nature, 249*(5456), 488–490.

Blakemore, C., & Sutton, P. (1969). Size adaptation: A new aftereffect. *Science, 166* (3902), 245–247.

Brainard, D. H. (1997). The psychophysics Toolbox. *Spatial vision, 10*(4), 433–436.

Camp, A. J., Tailby, C., & Solomon, S. G. (2009). Adaptable mechanisms that regulate the contrast response of neurons in the primate lateral geniculate nucleus. *Journal of Neuroscience, 29*(15), 5009–5021.

Dao, D. Y., Lu, Z. L., & Dosher, B. A. (2006). Adaptation to sine-wave gratings selectively reduces the contrast gain of the adapted stimuli. *Journal of Vision, 6*(7), 6.

Daumail, L., Carlson, B. M., Mitchell, B. A., Cox, M. A., Westerberg, J. A., Johnson, C., & Dougherty, K. (2023). Rapid adaptation of primate LGN neurons to drifting grating stimulation. *Journal of Neurophysiology, 129*(6), 1447–1467.

De Valois, R. L., Abramov, I., & Jacobs, G. H. (1966). Analysis of response patterns of LGN cells. *Journal of the optical Society of America, 56*(7), 966–977.

Derrington, A. M., & Lennie, P. (1984). Spatial and temporal contrast sensitivities of neurones in lateral geniculate nucleus of macaque. *The Journal of physiology, 357*(1), 219–240.

Derrington, A. M., Krauskopf, J., & Lennie, P. (1984). Chromatic mechanisms in lateral geniculate nucleus of macaque. *The Journal of Physiology, 357*(1), 241–265.

Edwards, M., Goodhew, S. C., & Badcock, D. R. (2021). Using perceptual tasks to selectively measure magnocellular and parvocellular performance: Rationale and a user's guide. *Psychonomic Bulletin & Review, 28*, 1029–1050.

Falconbridge, M., Ware, A., & MacLeod, D. I. (2010). Imperceptibly rapid contrast modulations processed in cortex: Evidence from psychophysics. *Journal of Vision, 10* (8), 21.

Gibson, J. J. (1933). Adaptation, after-effect and contrast in the perception of curved lines. *Journal of Experimental Psychology, 16*(1), 1.

Gori, S., Seitz, A. R., Ronconi, L., Franceschini, S., & Facoetti, A. (2016). Multiple causal links between magnocellular–dorsal pathway deficit and developmental dyslexia. *Cerebral cortex, 26*(11), 4356–4369.

Gouras, P., & Zrenner, E. (1979). Enhancement of luminance flicker by color-opponent mechanisms. *Science, 205*(4406), 587–589.

Hammett, S. T., & Smith, A. T. (1992). Two temporal channels or three? *A re-evaluation. Vision Research, 32*(2), 285–291.

Hawken, M. J., Shapley, R. M., & Grosof, D. H. (1996). Temporal-frequency selectivity in monkey visual cortex. *Visual neuroscience, 13*(3), 477–492.

Hisakata, R., & Kaneko, H. (2021). Temporal enhancement of cross-adaptation between density and size perception based on the theory of magnitude. *Journal of Vision, 21* (11), 11.

Hisakata, R., Nishida, S. Y., & Johnston, A. (2016). An adaptable metric shapes perceptual space. *Current Biology, 26*(14), 1911–1915.

Jiang, Y., Zhou, K., & He, S. (2007). Human visual cortex responds to invisible chromatic flicker. *Nature nNeuroscience, 10*(5), 657–662.

Johnston, A., & Clifford, C. W. G. (1995). A unified account of three apparent motion illusions. *Vision Research, 35*(8), 1109–1123.

Johnston, A., Bruno, A., Watanabe, J., Quansah, B., Patel, N., Dakin, S., & Nishida, S. Y. (2008). Visually-based temporal distortion in dyslexia. *Vision research, 48*(17), 1852–1858.

Johnston, A., McOwan, P. W., & Benton, C. P. (1999). Robust velocity computation from a biologically motivated model of motion perception. *Proceedings of the Royal Society of London. Series B: Biological Sciences, 266*(1418), 509–518.

Jovanovic, L., McGraw, P. V., Roach, N. W., & Johnston, A. (2022). The spatial properties of adaptation-induced distance compression. *Journal of Vision, 22*(11), 7.

Kaiser, P. K., Lee, B. B., Martin, P. R., & Valberg, A. (1990). The physiological basis of the minimally distinct border demonstrated in the ganglion cells of the macaque retina. *The Journal of Physiology, 422*(1), 153–183.

Kassambara, A. (2019). *rstatix: Pipe-friendly framework for basic statistical tests*. CRAN: Contributed Packages.

Kay, M., Elkin, L., Higgins, J., Wobbrock, J. (2025). ARTool: Aligned Rank Transform for Nonparametric Factorial ANOVAs. doi:10.5281/zenodo.594511, R package version 0.11.2, https://github.com/mjskay/ARTool.

Kelly, D. H. (1983). Spatiotemporal variation of chromatic and achromatic contrast thresholds. *Journal of the Optical Society of America, 73*(6), 742–750.

Kleiner, M., Brainard, D., Pelli, D., (2007). "What's new in Psychtoolbox-3?" Perception 36 ECVP Abstract Supplement.

Köhler, W., & Wallach, H. (1944). Figural after-effects. an investigation of visual processes. *Proceedings of the American Philosophical Society, 88*(4), 269–357.

Kulikowski, J. J., & Tolhurst, D. J. (1973). Psychophysical evidence for sustained and transient detectors in human vision. *The Journal of Physiology, 232*(1), 149–162.

Lambert, A., Wells, I., & Kean, M. (2003). Do isoluminant color changes capture attention? *Perception & Psychophysics, 65*, 495–507.

Lee, B. B., & Sun, H. (2009). The chromatic input to cells of the magnocellular pathway of primates. *Journal of Vision, 9*(2), 15.

Lee, B. B., Martin, P. R., & Valberg, A. (1988). The physiological basis of heterochromatic flicker photometry demonstrated in the ganglion cells of the macaque retina. *The Journal of Physiology, 404*(1), 323–347.

Lee, B. B., Pokorny, J., Smith, V. C., Martin, P. R., & Valbergt, A. (1990). Luminance and chromatic modulation sensitivity of macaque ganglion cells and human observers. *Journal of the Optical Society of America A, 7*(12), 2223–2236.

Legge, G. E. (1978). Sustained and transient mechanisms in human vision: Temporal and spatial properties. *Vision Research, 18*(1), 69–81.

Linares, D., & López-Moliner, J. (2016). quickpsy: An R package to fit psychometric functions for multiple groups.

Livingstone, M. S., & Hubel, D. H. (1987). Psychophysical evidence for separate channels for the perception of form, color, movement, and depth. *Journal of Neuroscience, 7* (11), 3416–3468.

Makowski, D., Ben-Shachar, M. S., Patil, I., & Lüdecke, D. (2020). Methods and algorithms for correlation analysis in R. *Journal of Open Source Software, 5*(51), 2306.

Mandler, M. B., & Makous, W. (1984). A three channel model of temporal frequency perception. *Vision research, 24*(12), 1881–1887.

McKeefry, D. J., Laviers, E. G., & McGraw, P. V. (2006). The segregation and integration of colour in motion processing revealed by motion after-effects. *Proceedings of the Royal Society B: Biological Sciences, 273*(1582), 91–99.

McGraw, P. V., McKeefry, D. J., Whitaker, D., & Vakrou, C. (2004). Positional adaptation reveals multiple chromatic mechanisms in human vision. *Journal of Vision, 4*(7), 8.

Merigan, W. H., & Maunsell, J. H. (1993). How parallel are the primate visual pathways? *Annual Review of Neuroscience, 16*, 369–402. https://doi.org/10.1146/annurev.ne.16.030193.002101

Nealey, T. A., & Maunsell, J. H. (1994). Magnocellular and parvocellular contributions to the responses of neurons in macaque striate cortex. *Journal of Neuroscience, 14*(4), 2069–2079.

Pelli, D. G. (1997). The VideoToolbox software for visual psychophysics: Transforming numbers into movies. *Spatial Vision, 10*, 437–442.

Raghavan, R. T., Kelly, J. G., Hasse, J. M., Levy, P. G., Hawken, M. J., & Movshon, J. A. (2023). Contrast and luminance gain control in the macaque's lateral geniculate nucleus. *ENeuro, 10*(3).

Robinson, J. O. (1972). *The psychology of visual illusion*. Hutchinson University Library.

Schiller, P. H., & Colby, C. L. (1983). The responses of single cells in the lateral geniculate nucleus of the rhesus monkey to color and luminance contrast. *Vision Research, 23* (12), 1631–1641.

Shady, S., MacLeod, D. I., & Fisher, H. S. (2004). Adaptation from invisible flicker. *Proceedings of the National Academy of Sciences, 101*(14), 5170–5173.

Smith, G. J., & Henriksson, M. (1955). The effect on an established percept of a perceptual process beyond awareness. *Nordisk Psykologi, 7*(3–4), 170–179.

Solomon, S. G. (2021). *Retinal ganglion cells and the magnocellular, parvocellular, and koniocellular subcortical visual pathways from the eye to the brain. In Handbook of clinical neurology* (Vol. 178,, 31–50.

Solomon, S. G., Peirce, J. W., Dhruv, N. T., & Lennie, P. (2004). Profound contrast adaptation early in the visual pathway. *Neuron, 42*(1), 155–162.

Stein, J. (2019). The current status of the magnocellular theory of developmental dyslexia. *Neuropsychologia, 130*, 66–77.

Stein, J., & Walsh, V. (1997). To see but not to read; the magnocellular theory of dyslexia. *Trends in Neurosciences, 20*(4), 147–152.

Tagoh, S., Hamm, L. M., Schwarzkopf, D. S., & Dakin, S. C. (2022). Motion adaptation improves acuity (but perceived size doesn't matter). *Journal of Vision, 22*(11), 2.

Tailby, C., Solomon, S. G., Dhruv, N. T., Majaj, N. J., Sokol, S. H., & Lennie, P. (2007). A new code for contrast in the primate visual pathway. *Journal of Neuroscience, 27* (14), 3904–3909.

Vul, E., & MacLeod, D. I. (2006). Contingent aftereffects distinguish conscious and preconscious color processing. *Nature Neuroscience, 9*(7), 873–874.

Watson, A. B., & Pelli, D. G. (1983). QUEST: A Bayesian adaptive psychometric method. *Perception & Psychophysics, 33*(2), 113–120.

Webster, M. A., De Valois, K. K., & Switkes, E. (1990). Orientation and spatial-frequency discrimination for luminance and chromatic gratings. *Journal of the Optical Society of America A, 7*(6), 1034–1049.

Wobbrock, J. O., Findlater, L., Gergle, D., & Higgins, J. J. (2011). May). the aligned rank transform for nonparametric factorial analyses using only anova procedures. In *In Proceedings of the SIGCHI conference on human factors in computing systems* (pp. 143–146).

Yeh, S. L., Chen, I., De Valois, K. K., & De Valois, R. L. (1996). Figural aftereffects and spatial attention. *Journal of Experimental Psychology: Human Perception and Performance, 22*(2), 446.

Yoshioka, T., Levitt, J. B., & Lund, J. S. (1994). Independence and merger of thalamocortical channels within macaque monkey primary visual cortex: Anatomy of interlaminar projections. *Visual Neuroscience, 11*(3), 467–489.

Zhuang, X., Pokorny, J., & Cao, D. (2015). Flicker adaptation desensitizes the magnocellular but not the parvocellular pathway. *Investigative Ophthalmology & Visual Science, 56*(5), 2901–2908.

Zimmermann, E. (2023). *Repulsive aftereffects of visual space. Vision, 7*(4), 73.